Detecting Strata Fracturing and Roof Failures from a Borehole Based Microseismic System

T. S. Bajpayee, Lead Research Engineer
A. T. Iannacchione, Principal Research Engineer
NIOSH-Pittsburgh Research Laboratory
Pittsburgh, PA

S. R. Schilling, UG Mine Engineer/Geologist
Pleasant Gap Mine
Pleasant Gap, PA

ABSTRACT

Modern, highly productive underground mining operations need to assure the safety of their workforce by understanding where major strata fractures and roof failures could occur. Mines depend on a host of tools to assess ground instability. In-mine microseismic monitoring systems with sufficient number of sensors have also been used to provide this information. These in-mine systems must be robust in design and moved regularly to keep up with the mining advancement. System performance issues depend on maintaining ever increasing cable runs, preventing component damage from mining activities (scaling, blasting, etc.) and avoiding signal degradation due to interference from mining equipment (fans, trucks, electrical equipment, etc.). A potential solution is to use a surface-based monitoring system having sensors placed in boreholes above and adjacent to the underground mine workings. These sensors must be capable of detecting and locating strata fracturing associated with rock failure events. A great advantage of a surface-based monitoring system is its independence from the underground mine infrastructure. There is less concern with cable maintenance problems, signal degradation by interference from mining activity, or loss of power from the mine's power grid. The disadvantages include the cost of drilling boreholes and challenges associated with placing sensors in the boreholes, maintaining radio communication and solar power, and public interference (vandalism, etc.).

This paper describes a case study where a surface-based microseismic system, using triaxial geophones in boreholes drilled from the surface, was deployed at a large limestone mine. The system was operational during a roof fall that occurred in October 2007. It detected the first rock fracture event 17 minutes before the rock fall event. The geophone array was sensitive enough to identify all large rock fracture, impact, and blast events as well as medium-size rock fracture events occurring close to the geophone array.

INTRODUCTION AND BACKGROUND

Falls of ground represent one of the most significant hazards to our nation's miners. Accidental deaths due to falls of ground account for 43% of all underground mining fatalities (NIOSH, 2004). Reducing the number of ground fall injuries is a central goal of the National Institute for Occupational Safety and Health (NIOSH) mine safety research program. This study constitutes a part of the research goal of reducing injuries due to ground failure in the mining industry. A small but growing segment of the mining industry is underground stone. Generally, entries in stone mines have heights ranging from 6.1 m (20 ft) to 18.3 m (60 ft) that make it more difficult to quickly recognize deteriorating roof conditions. This study evaluates a surface-based microseismic system for monitoring rock fracturing and roof fall events at an underground stone mine in central Pennsylvania.

Applications of microseismic systems to monitor roof stability have been examined by the underground mining sector. This technology has been used in many countries notably Australia, Canada, South Africa, United Kingdom, and the United States to monitor ground stability issues. An early evaluation of this technology by Obert and Duvall (1945a and 1945b) dates back to the 1940's. When a roof rock fractures or moves along a slip plane, it typically emits microseismic emissions. Miners have often noticed the association of popping or cracking noises with fracturing of roof strata. Obert and Duvall (1967) have long recognized that for every audible noise, there most likely occurs an equivalent multitude of microseismic emissions. Each of these emissions signifies the formation of a new rupture surface or slip on an existing fracture surface. Development of new fractures can lower the overall rock mass strength (Hardy, 1975). Therefore, elevated levels of seismicity generally signal development of potentially unstable strata conditions (Brady and Haramy, 1994).

During the past decade, microseismic monitoring techniques to characterize roof instability have been reported by Hayes (2000), Cai et al. (2001), Heasley et al. (2001), Iannacchione et al. (2004, 2005), and Srinivasan et al. (2005). More recently, Ellenberger and Bajpayee (2007) studied the application of microseismic monitoring techniques for early detection of roof instability.

A seismic event due to rock fracturing generates transient dynamic elastic waves that propagate through the surrounding rock mass. The p- and s-waves, also known as body waves, travel in a rock medium at characteristic velocities, C_p and C_s, given by the following equations (Persson et al., 1993), where C_p is the p-wave velocity (m/s), C_s is the s-wave velocity (m/s), E is the

modulus of elasticity (GPa), v is the Poisson's ratio, and ρ is the density (kg/m^3) of the medium.

$$C_p = \left[\frac{E(1-v)}{(1+v)(1-2v)\rho} \right]^{1/2} \qquad (1)$$

$$C_s = \left[\frac{E}{2(1+v)\rho} \right]^{1/2} \qquad (2)$$

Wave velocities at this study site were determined using several test blasts. The average value of the p-wave velocity was 6,039 m/s (19,813 ft/s) and for the s-wave 3,017 m/s (9,899 ft/s). These values were used for computing source location.

Mining-induced microseismicity generally relates to shear and tensile fractures in a rock mass caused by normal mining operations. Five modes of failure examined by Gale et al. (2001) are: (1) shear fracture through intact rock material, (2) tensile fracture through intact rock material, (3) shear fracture of bedding planes, (4) tensile fracture of bedding, and (5) remobilization of pre-existing fractures. While the seismic waves due to shear fractures could literally propagate hundreds of meters, the seismic waves due to low-energy tensile failures rarely propagate beyond the first hundred meters. Low-energy tensile failures are difficult to locate unless the event is close to the seismic array.

A borehole-based microseismic monitoring system was installed from the surface of a large underground stone mine in Center County, Pennsylvania with the objectives of:

- increasing fundamental knowledge of roof behavior in a room-and-pillar stone mining operation,
- evaluating a surface-based rock fracture and roof fall detection technology, and
- examining the location and extent of roof instability prior to failure.

This project is a cooperative effort between NIOSH and the operator of a large underground stone mine. NIOSH provided most of the data acquisition and monitoring instrumentation. The mine operator provided access to its site, necessary infrastructure, cost of drilling and maintaining boreholes, central data acquisition and processing computer, and support of other operational requirements.

GEOLOGIC SETTING AND MINING CONDITIONS

The study mine is extracting limestone by underground room-and-pillar mining in the Valentine member of the Linden Hall formation belonging to the Lower Middle Ordovician Limestones (Rones, 1969). The Valentine member is about 22.9 m (75 ft) thick in this area and comprises rocks of two closely related lithologic types. The upper 15.2 m (50 ft) comprises unlaminated, light-gray calcilutites ranging from 0.9 to 1.5 m (3 to 5 ft) in thickness (Rones, 1969). The lower 6.1 m (20 ft) is well laminated with thickness ranging from 0.3 to 0.9 m (1 to 3 ft) with thin clay or fine bentonite partings. The Valentine Limestone comprising light-gray, chemically pure limestone lies above the dark-gray 12.8-m (42-ft)-thick Valley View member of the Linden Hall formation. About 9.1 m (30 ft) of dark-gray and thinly-bedded section of Centre Hall member of the Nealmont formation lies above the Valentine Limestone. The Valentine Limestone generally dips at 15 degrees and the strike direction runs approximately at N60°E (Rones, 1969).

The southward advance of mining is projected to extend below the Nittany mountain range to a depth of about 549 m (1800 ft). The uniaxial compressive strength of Valentine Limestone ranges from 100 to 145 MPa (14,500 to 21,000 psi) and the maximum horizontal stress from 14.9 to 29.6 MPa (2,170 to 4,300 psi) in the N80°E direction (Esterhuizen and Iannacchione, 2004). The elastic modulus of Valentine Limestone is about 50 GPa (7.25x10^6 psi).

The mine management adopted a novel stress control mine design to alleviate the effects of high horizontal stress and improve ground stability. Pillars are rectangular having their long axis oriented parallel to the maximum horizontal stress direction. Pillar size is approximately 46 x 20 m (150 x 65 ft). The percentage of extraction is roughly 60% with 40% left in pillars to support the superincumbent strata. Crosscuts are staggered to develop three-way intersections. During development, rooms are driven to 15.2 m (50 ft) wide by 7 m (23 ft) high using 4.4-m (14-ft) deep wedge pattern blast holes. Subsequently, an additional 11.3 m (37 ft) of rock is extracted by floor-benching. The overburden thickness ranges from outcrop to approximately 274.3 m (900 ft). Figure 1 shows the benched and development areas in relation to boreholes A, B, C, and D where seismic sensors are installed.

The dark-gray, thin-bedded Centre Hall Limestone immediately above the Valentine is laminated and not strong enough to constitute the immediate roof beam. On the other hand, Valentine Limestone is massive and strong to form a stable roof beam. In areas where the mining depth exceeds 274.3 m (900 ft), a layer of Valentine Limestone of thickness 1.8 m (6 ft) or more is left at the top of the entry to act as an immediate roof beam. In addition, a stable roof profile is maintained, where possible, by implementing controlled blasting using emulsion explosives with non-electric delay detonators. A significant outcome is enhanced ground stability, reduction of guttering, and diminution of roof fractures and roof failures. Good ground control measures are used at this mine to ensure long-term stability of entries, particularly entries related to haulage, ventilation, and escape ways. Implementation of a safety culture, since the operations began in June 1998, has contributed to prevention of fatal ground-fall injuries. Additionally, no lost-day injuries were attributed to roof fall events since 2001.

MICROSEISMIC SYSTEM DESCRIPTION

A surface-based microseismic monitoring system developed and marketed by Engineering Seismology Group[1] (ESG), Canada was installed at the study mine. During the initial drilling phase, two boreholes collapsed prior to installing any geophones. The presence of a Bentonite layer in the overburden most likely caused the borehole collapse. New holes were drilled in different locations and geophones were successfully installed. Eight triaxial geophones were installed in four deep boreholes drilled from the surface. Table 1 lists the depth of the Valentine roof level below the sensor location. This depth ranged from 9.2 m (30.2 ft) to 175.4 m (575.3 ft). Borehole B extends about 297.3 m (975.3 ft) below the surface level.

The microseismic system consists of a central site located at the mine office and four borehole sites distributed over the current and projected mining progression areas. At each borehole site, a

---

[1] Mention of any company or product does not constitute endorsement by the National Institute for Occupational Safety and Health..
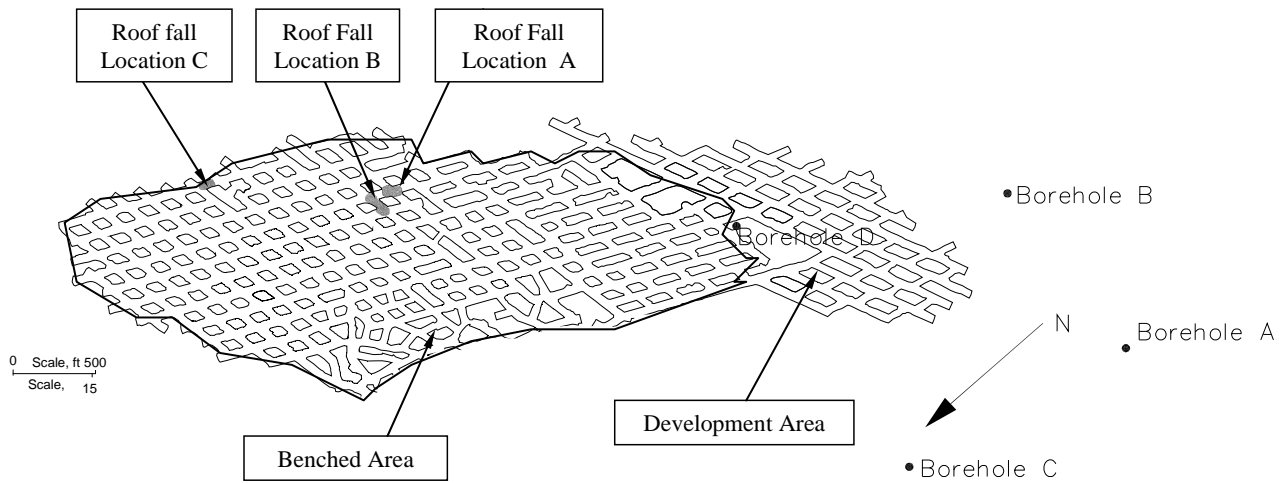
Figure 1. Roof fall areas and borehole locations on a mine map.

Table 1. Depth of Valentine Limestone below seismic sensors (triaxial geophones).

Borehole ID	Sensor ID	Depth of Valentine roof below sensor location, m (ft)	Depth of sensor below the surface level, m (ft)
A	Sensor 1	99.8 (327.4)	76.5 (251.0)
A	Sensor 2	130.6 (428.4)	45.7 (150.0)
B	Sensor 1	144.9 (475.3)	152.4 (500.0)
B	Sensor 2	175.4 (575.3)	121.9 (400.0)
C	Sensor 1	9.2 (30.2)	110.9 (364.0)
C	Sensor 2	39.7 (130.2)	80.5 (264.0)
D	Sensor 1	85.0 (279.0)	152.4 500.0)
D	Sensor 2	115.5 (379.0)	121.9 (400.0)

Figure 2. Microseismic data acquisition station at a borehole site.

Figure 3. Cables leading from the geophones to the data acquisition processor.

local data acquisition station (figure 2) is set up with its processor unit, power supply, radio communication, GPS timing, and geophones. Two geophones and associated data transfer cables were carefully handled and placed in the borehole (figure 3). The cable ends were then connected to the local data acquisition station.
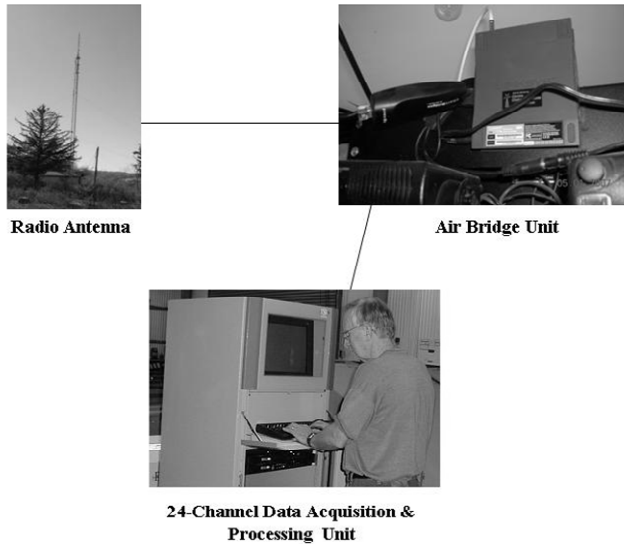
The computer at the central site is running a network data acquisition system for real time data acquisition and processing by interfacing with the four borehole stations using TCP/IP communications. The essential system components at the central site are shown in figure 4. The central site controls each borehole site and continuously monitors all 24-channels of the seismic array. Event triggering is controlled by setting limits for individual channels.

Figure 4. Essential system components at the central site.

Each borehole data acquisition station is powered by six, 12-volt, rechargeable batteries. A twin-unit solar panel recharges the battery pack. The solar panel is mounted on the roof of the instrument housing (figure 2). Each borehole station has 2 GB internal storage capacity and is a web-enabled microseismic recorder/server with a sampling rate from 50 Hz to 10 kHz. The sampling rate during this study was 4 kHz. The essential system components of a borehole site are shown in figure 5. Each borehole data acquisition and processor station communicates with two attached triaxial geophones and the GPS receiver-timing unit. Each timing unit receives a time signal from the GPS and transfers the data to the system so that all four borehole stations are synchronized and record seismic signals on a common time base. Eight triaxial geophones, each capable of measuring seismic wave in three perpendicular directions, are installed in four boreholes (figure 1).
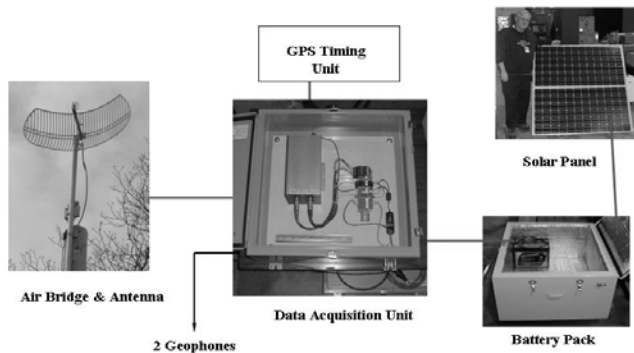
Figure 5. Essential system components at a borehole site.

OCTOBER 2007 ROOF FALL

A roof fall occurred during the afternoon of October 22, 2007, in an abandoned part of the mine. During a routine afternoon inspection, an unusually high concentration of air-borne dust near the southeast end of the mine was observed. As the inspection progressed, it was observed that several brattices in the area were

knocked down. These two observations indicated that an air-blast had been produced due to a roof fall. Upon further examination, it was observed that an entire intersection of roof at location A (figure 1) had fallen. The intersection area from the bottom of the benched floor to the top of the roof-line was filled with fallen roof debris. It is estimated that the roof cavity extended about 18 m (60 ft) or more above the normal roof-line. An estimated 31,000 tons of roof rock had fallen in this intersection.

It was further noticed that another intersection, location B (figure 1), had also collapsed and the debris completely filled the entire height from the bottom of the benched floor to the visible roof-line. The condition of this intersection was similar to the intersection at location A. The pillars around these two fall areas were intact and did not show any signs of degradation due to the impact of falling roof debris or stress redistribution pursuant to the roof falls. These 4-way intersections were drifted in November 2001 and benched in June 2006. About 12-ft of immediate roof layer further to the northeast of these falls, location C, had also collapsed (figure 1). This fall was about 29 m (95 ft) long and covered the entire width of the entry. Roof fall areas in locations A, B, and C were abandoned and bermed off in July 2006.

## Microseismicity Associated with the October 2007 Roof Fall

The background seismicity rate prior to the October 22 roof fall was about two events per day. Figure 6 shows a plot of thirty five rock fracture events recorded during this roof fall episode. The first rock fracture event was recorded at 1:37 PM on October 22 and within a period of 17 minutes another eight rock fracture events were recorded. Thereafter, the event rate slowed down. It resurged at 1:33 PM on October 23 and fifteen events were recorded within a period of about 1 hour and 11 minutes. Later, the microseismicity rate returned to the background level.
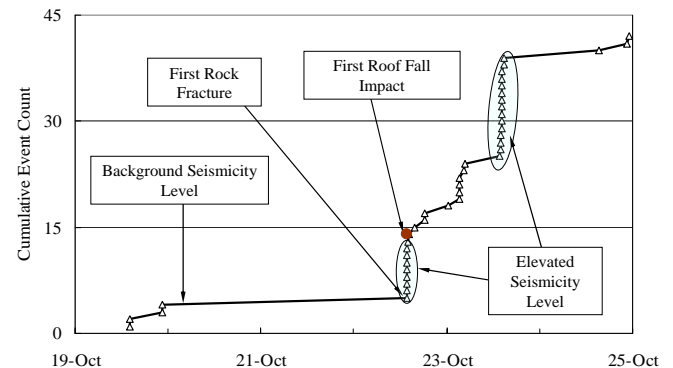
**Figure 6. Cumulative plot of rock fracture events.**

Roof fall impact signatures are different from rock fracture signatures. Generally, rock fracture signatures display sharp p- and s-arrivals and the wave amplitude generally decays rapidly within a fraction of a second. The rock fracture event shown in figure 7 lasted for about 275 ms and the maximum particle velocity recorded was 0.05 mm/s. A spectral analysis of the rock fracture waveform using the ESG software yielded a corner frequency of 75 Hz. The amplitude diminished rapidly for all frequencies over 75 Hz. Roof fall impact signatures are long emergent waves of generally more than a second in duration. The roof fall impact event shown in figure 8 essentially represents a s-

wave signature. It is characterized by a duration of about 3 sec, maximum particle velocity of 0.2 mm/s, and a corner frequency of 22 Hz. Exact location and source parameters of impact events are difficult to calculate due to the emergent nature of the wave. The first roof fall impact signature was observed at 1:54 PM on October 22. Two more roof fall impacts quickly followed the first impact. Another three roof fall impacts were observed much later on October 22. Currently, plans are being finalized to install additional sensors to extend seismic coverage area and enhance array sensitivity.
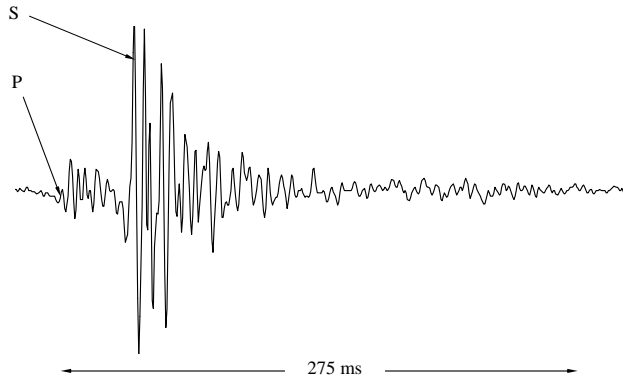
Figure 7. Seismic signature of a rock fracture event showing p-and s-wave arrivals.

SUMMARY AND CONCLUSIONS
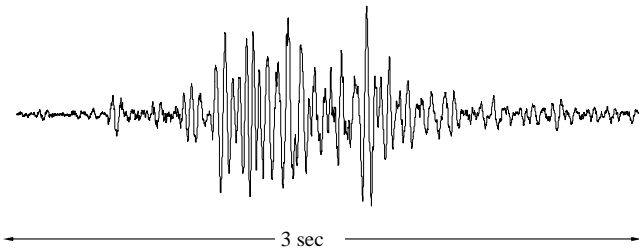
Figure 8. Seismic signature of an impact event.

Falls of ground represent a great hazard for the miners in underground situations, particularly in stone mines where entry heights range from 6.1 m (20 ft) to 18.3 m (60 ft). Microseismic monitoring is another tool to anticipate roof fall hazards by assessing stability conditions in underground stone mines. In-mine seismic monitoring has been used to warn miners about potential roof instability in other types of mining, and the goal here is to apply this technology to the underground stone mining sector.

A surface-based system comprising eight triaxial geophones is installed at a large stone mining operation conducting room-and-pillar mining. The system is self-contained and does not depend on an underground power grid. The monitoring system detected elevated level of microseismicity during a large roof fall that occurred in an abandoned part of the mine. The system detected the first elevated microseismic event 17 minutes before the first rock fall. The monitoring system displayed a marked increase in the seismicity level from the background rate (2 events per day) during the roof fall episode. Plans are underway to install additional geophones to extend the seismic coverage area and improve array sensitivity. NIOSH plans to continue this study to

further evaluate the relationship between microseismicity and roof instability.

DISCLAIMER

The findings and conclusions in this paper have not been formally disseminated by the National Institute for Occupational Safety and Health and should not be construed to represent any agency determination or policy.

REFERENCES

1. **Brady, B.T. and Haramy, K.Y.,** (1994). High Amplitude Stress Wave Generation and Damage Induced by Roof Caving in Mines. Proceedings of the First North American Rock Mechanics Symposium, Austin, TX, pp. 1033-1040.

2. **Cai, M., Kaiser, P.K. and Martin, C.D.,** (2001). Quantification of Rock Mass Damage in Underground Excavations from Microseismic Event Monitoring. International Journal of Rock Mechanics and Mining Sciences *38*:1135-1145.

3. **Ellenberger, J.L. and Bajpayee, T.S.,** (2007). An Evaluation of Microseismic Activity Associated with Major Roof Falls in a Limestone Mine: A Case Study. 2007 SME Annual Meeting and Exhibit, Denver, Colorado, preprint 07-103, pp. 1-5.

4. **Esterhuizen, G.S. and Iannacchione, A.T.,** (2004). Investigation of Pillar-Roof Contact Failure in Northern Appalachian Stone Mine Workings. Proceedings of the 23rd International Conference on Ground Control in Mining, Morgantown, WV, pp. 320-326.

5. **Gale, W.J., Heasley, K.A., Iannacchione, A.T., Swanson, P.L., Heatherly, P. and King, A.,** (2001). Rock Damage Characterization from Microseismic Monitoring. Proceedings of the 38th U.S. Rock Mechanics Symposium, Washington, D.C.

6. **Hardy, R.,** (1975). Emergence of AE/MA as a Tool in Geomechanics. Proceedings of the First Conference on Acoustic Emission-Microseismic Activity in Geologic Structures and Materials, University Park, PA, June 9-11, Series on Rock and Soil Mechanics *2*(3):13-31.

7. **Hayes, P.,** (2000). Moonee Colliery: Renewing the Economic Viability of a Mine Using Microseismic And Hydraulic Fracturing Techniques. Proceedings of the 19th International Conference on Ground Control in Mining, Morgantown, WV, pp. 38-44.

8. **Heasley, K.A., Ellenberger, J.L. and Jeran, P.W.,** (2001). ,Microseismics. Proceedings of the 20th International Conference on Ground Control in Mining, Morgantown, WV, pp. 280-286.

9. **Iannacchione, A.T., Coyle, P.R., Prosser, L.J., Marshall, T.E. and Listenberger, J.,** (2004). The Relationship of Roof Movement and Strata-Induced Microseismic Emissions to Roof Falls. 2004 SME Annual Meeting and Exhibit, Denver, Colorado, preprint 04-58, Littleton, CO, Society for Mining, Metallurgy, and Exploration, Inc., pp 1-9.

10 **Iannacchione, A.T., Esterhuizen, G.S., Bajpayee, T.S., Swanson, P.L. and Chapman, P.C.,** (2005). Characteristics of Mining-Induced Seismicity Associated With Roof Falls and Roof Caving Events. Proceedings of the 40th U.S. Rock Mechanics Symposium, Anchorage, AK, June 25-29 and American Rock Mechanics Association, Alexandria, VA, June 1-10.

11. **National Institute for Occupational Safety and Health (NIOSH)** (2004). Worker Health Chartbook. 2004 DHHS (NIOSH) Publication No. 2004-146, Washington, DC: US Department of Health and Human Services, Public Health Services, Centers for Disease Control and Prevention, National Institute for Occupational Safety and Health.

12. **Obert, L. and Duvall, W.I.,** (1945a). The Microseismic Method of Predicting Rock Failures in Underground Mining, Part 1, General Method. U. S. Bureau of Mines, RI 3797.

13. **Obert, L. and Duvall, W.I.,** (1945b). The Microseismic Method of Predicting Rock Failures in Underground Mining, Part 2, Laboratory Experiments. U. S. Bureau of Mines, RI 3803.

14. **Obert, L. and Duvall, W.I.,** (1967). Rock Mechanics and the Design of Structures in Rock. John Wiley and Sons, Inc., New York, NY, pp. 113-188.

15. **Persson, P., Holmberg, R. and Lee, J.,** (1993). Rock Blasting and Explosives Engineering. CRC Press, New York, NY, pp.342.

16. **Rones, M.,** (1969). A Lithostratigraphic, Petrographic and Chemical Investigation of the Lower Middle Ordovician Carbonate Rocks in Central Pennsylvania. General Geology Report G 53, Bureau of Topographic and Geologic Survey, Commonwealth of Pennsylvania.

17. **Srinivasan, C., Sivakumar, C., Gupta, R.N.,** (2005). Source Parameters of Seismic Events in a Coal Mine in India. 27th Seismic Research Review: Ground Based Nuclear Explosion Monitoring Technologies, Rancho Mirage, California, September, https://www.nemre.nnsa.doe.gov/review2005.